

Supporting Information for
A methodology to synthesize easily oxidized materials containing
Li ions in inert atmosphere

Itsuki Konuma¹, Yosuke Ugata^{1, 2}, and Naoaki Yabuuchi*^{1, 2}

¹Department of Chemistry and Life Science, Yokohama National University, 79-5

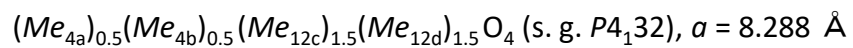
Tokiwadai, Hodogaya-ku, Yokohama 240-8501, Japan

²Advanced Chemical Energy Research Center (ACERC), Institute of Advanced
Sciences, Yokohama National University, 79-5 Tokiwadai, Hodogaya-ku, Yokohama
240-8501, Japan

*CORRESPONDING AUTHOR

E-mail: yabuuchi-naoaki-pw@ynu.ac.jp (Y.N.)

Table S1. Atomic positions of the cation-ordered rocksalt-type structure with space group $P4_132$ described in **Supporting Figure S3**.



	site	x	y	z	
	4a	cation	0.375	0.375	0.375
	4b	cation	0.875	0.875	0.875
	12c	cation	0.625	0.625	0.875
	12d	cation	0.125	0.125	0.375
	8c	anion	0.625	0.625	0.625
	24e	anion	0.875	0.875	0.625

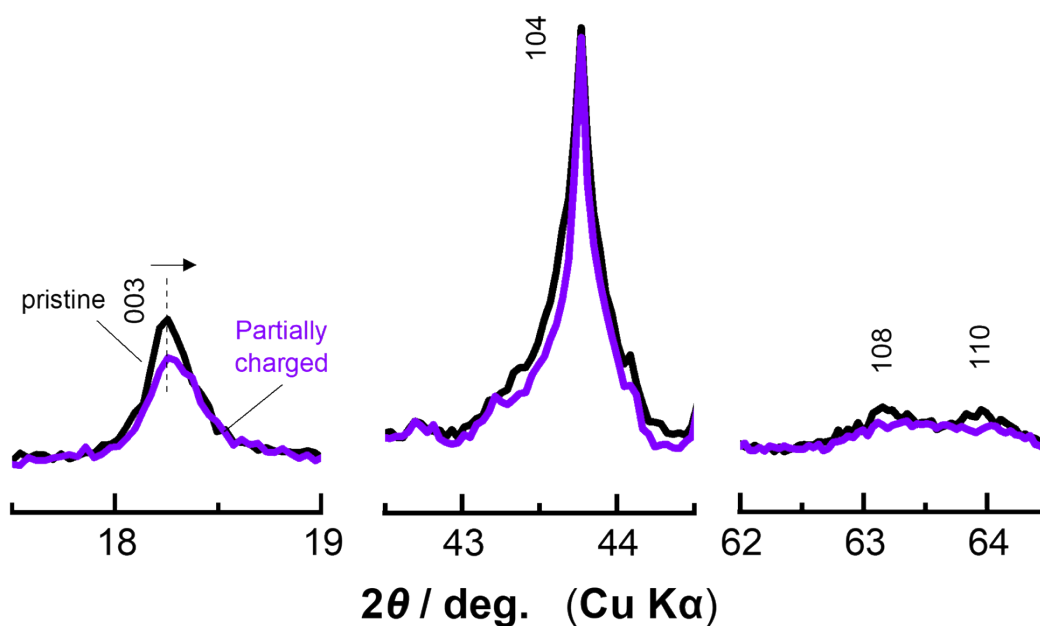
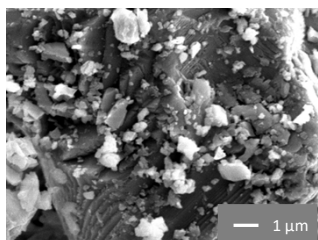


Figure S1. *In-situ* XRD patterns of nanosized $\text{Li}_{8/7-x}\text{Ti}_{2/7}\text{V}_{4/7}\text{O}_2$ prepared by ball milling at 450 rpm. The data of pristine and the delithiated sample after charge to 120 mA h g^{-1} are compared. The sample was charged at a rate of 30 mA g^{-1} at room temperature. After charging, A small peak shift to higher angle and decrease in intensity are observed in 003 diffraction line, and the peak splitting between 108 and 110 diffraction lines becomes less visible. In contrast, 104 diffraction line remains almost unchanged. These observations indicate the partial oxidation of V ions and the formation of cation-disordered rocksalt phase on charge. A similar trend is noted for the XRD pattern of the sample synthesized without Cu foil (**Figure 2a**), which suggests the formation of a Li deficiency phase because of partial oxidation of the sample by contaminated oxygen.

Ti-V with Cu



Ti-V without Cu

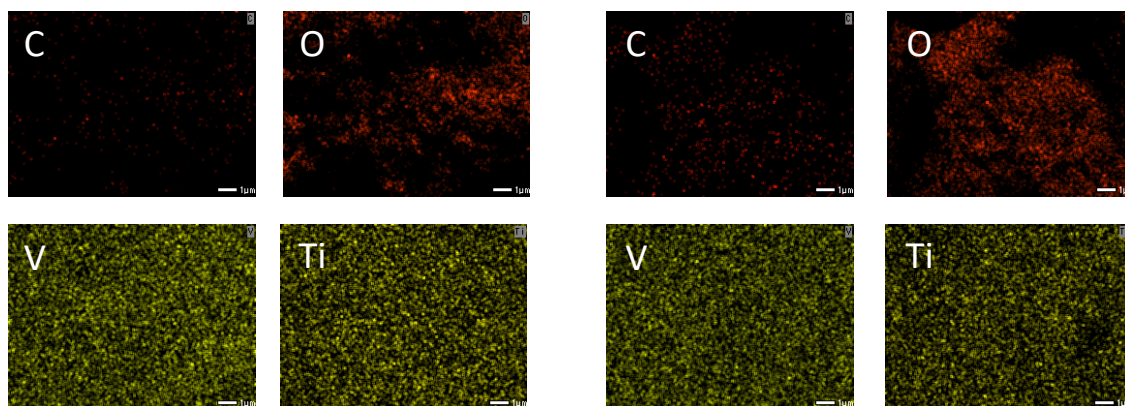
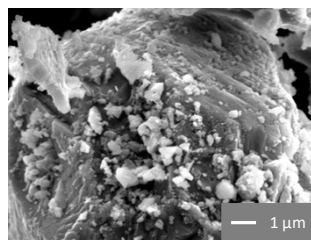


Figure S2. The SEM images and EDX mapping of $\text{Li}_{8/7}\text{Ti}_{2/7}\text{V}_{4/7}\text{O}_2$ synthesized with or without Cu foil. These data were collected using a scanning electron microscope (JSM-IT200, JEOL) operated at 10 kV.

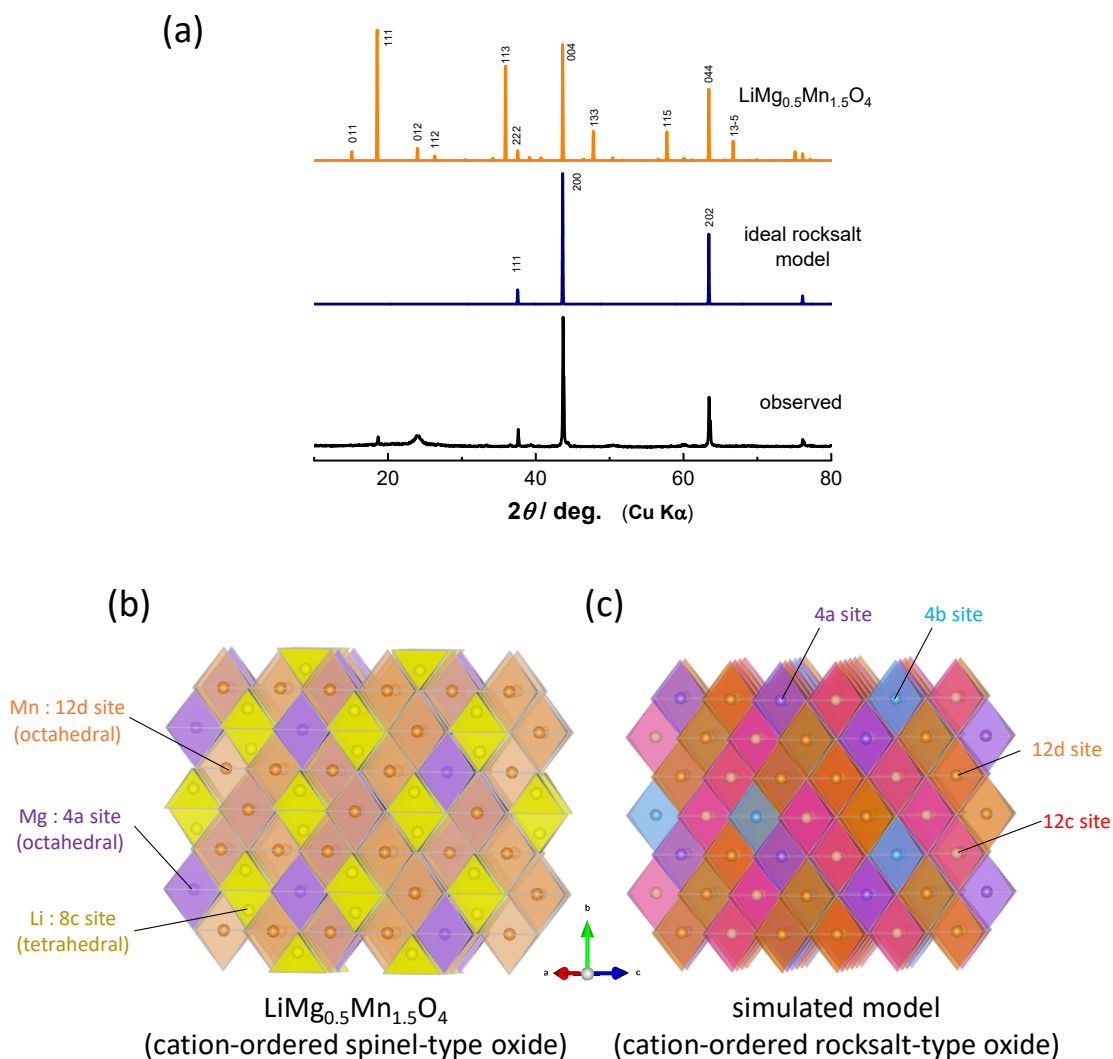


Figure S3. Analysis of additional peaks of $\text{Li}_{8/7}\text{Ti}_{2/7}\text{Mn}_{4/7}\text{O}_2$ synthesized without Cu foil by XRD simulation. A simulated model is derived from a cation-ordered spinel-type structure with a cubic symmetry. (a) Simulated XRD patterns of cation-ordered spinel-type $\text{LiMg}_{0.5}\text{Mn}_{1.5}\text{O}_4$, and an ideal cation-disordered rocksalt-type structure. The experimentally observed XRD pattern of $\text{Li}_{8/7}\text{Ti}_{2/7}\text{Mn}_{4/7}\text{O}_2$ synthesized without Cu foil is also shown for comparison. On the basis of cation-ordered model of $\text{LiMg}_{0.5}\text{Mn}_{1.5}\text{O}_4$ with space group $P4_132$ (b), tetrahedral 8c sites are replaced by octahedral 4b and 12c sites, forming a cation-ordered rocksalt structure (c). Atomic positions of the simulated model used for cation-ordered rocksalt structure with space group $P4_132$ are shown in **Table S1**.

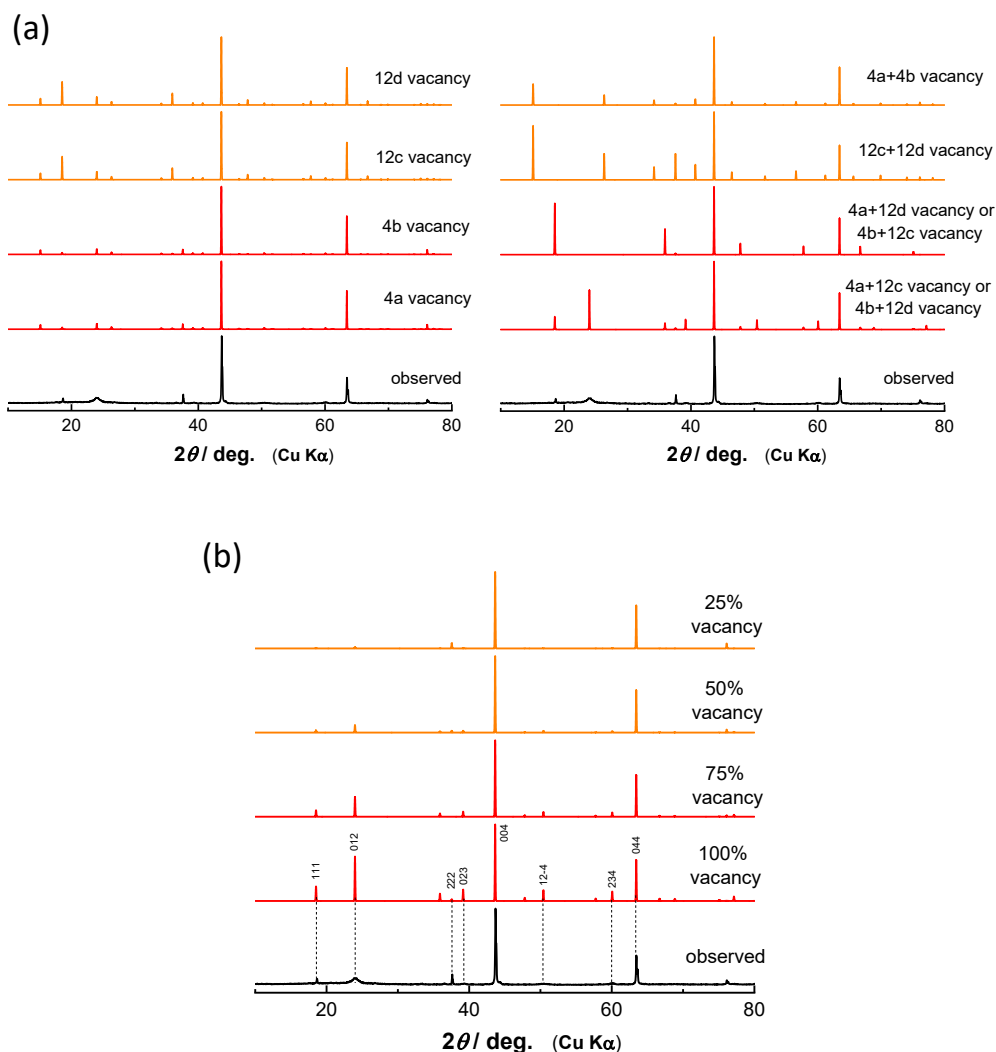


Figure S4. Simulated XRD patterns of the cation-ordered rocksalt structure with space group $P4_132$ shown in **Supporting Figure S3c**. Herein, the formation of vacant sites for different octahedral sites is considered and simulated in (a). In these models, all the occupied cation sites are assumed to be Al, which has the average atomic weight of cations in $\text{Li}_{8/7}\text{Ti}_{2/7}\text{Mn}_{4/7}\text{O}_2$. The positions of superlattice lines are reproduced compared with the experimental pattern when vacant sites are formed in both 4a and 12c sites (or 4b and 12d sites). The profile of diffraction pattern is well reproduced when the vacancy concentration at 4a and 12c sites is further optimized as shown in (b). The simulated XRD pattern with 50 % vacancy model shows a good matching with experimentally observed data. The broad peak at 24° is considered to originate from partial cation disordering based on the ideal model. This result suggests that approximately 25% octahedral vacancy is formed in $\text{Li}_{8/7}\text{Ti}_{2/7}\text{Mn}_{4/7}\text{O}_2$ synthesized without Cu foil if we assume that Li ordering is not present.

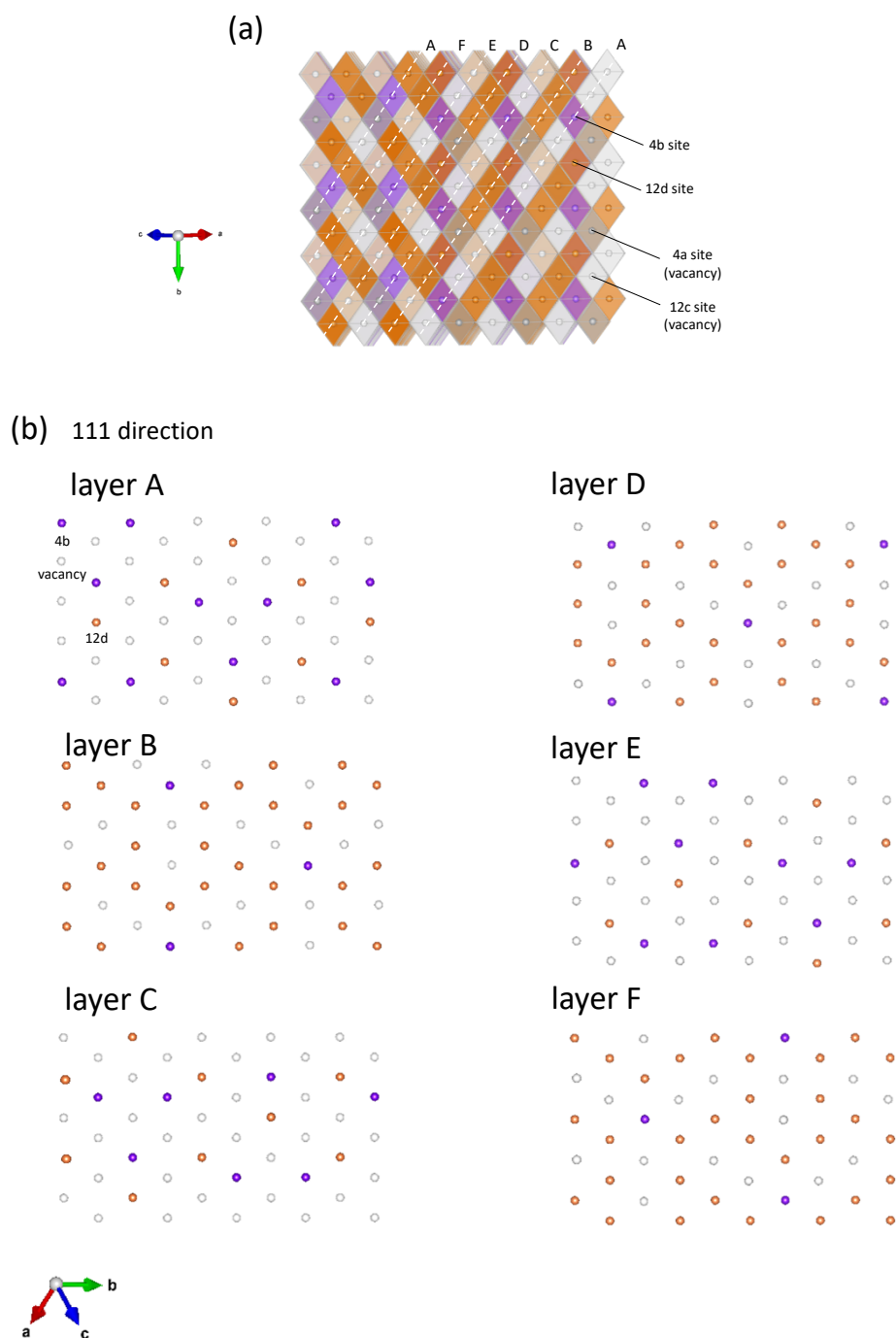
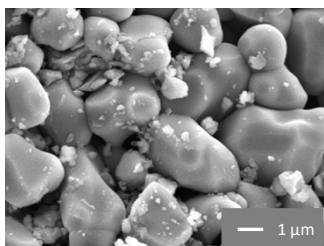


Figure S5. The cation and vacancy arrangements for the optimized structural model shown in **Supporting Figure S4b**. Partial cation vacancy is formed at 4a and 12c sites, and the schematic illustration of structural model along 011 direction (a). Cation and vacancy ordering along 111 direction is shown in (b). There are 6 types of different cation arrangements, layer A – F, in the structure.

Ti-Mn with Cu



Ti-Mn without Cu

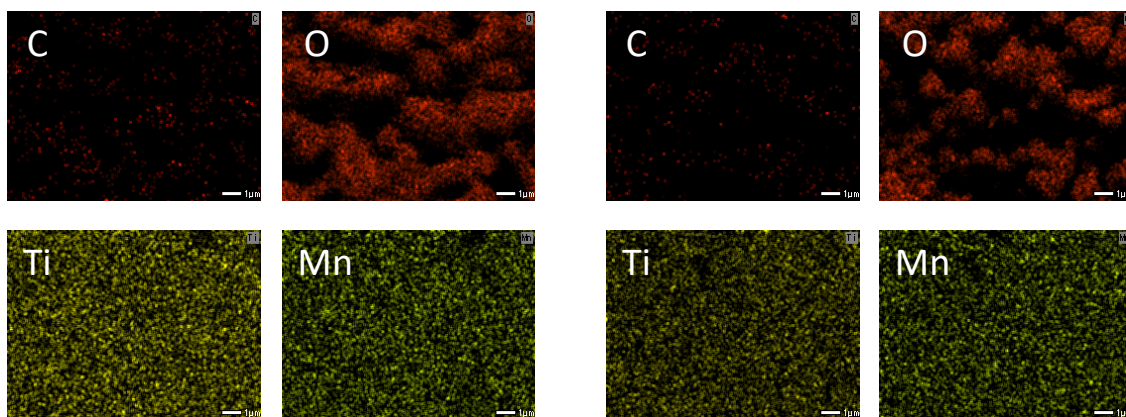
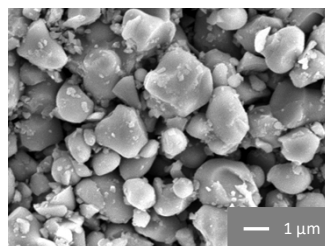


Figure S6. The SEM images and EDX mapping of $\text{Li}_{8/7}\text{Ti}_{2/7}\text{Mn}_{4/7}\text{O}_2$ with or without Cu foil.

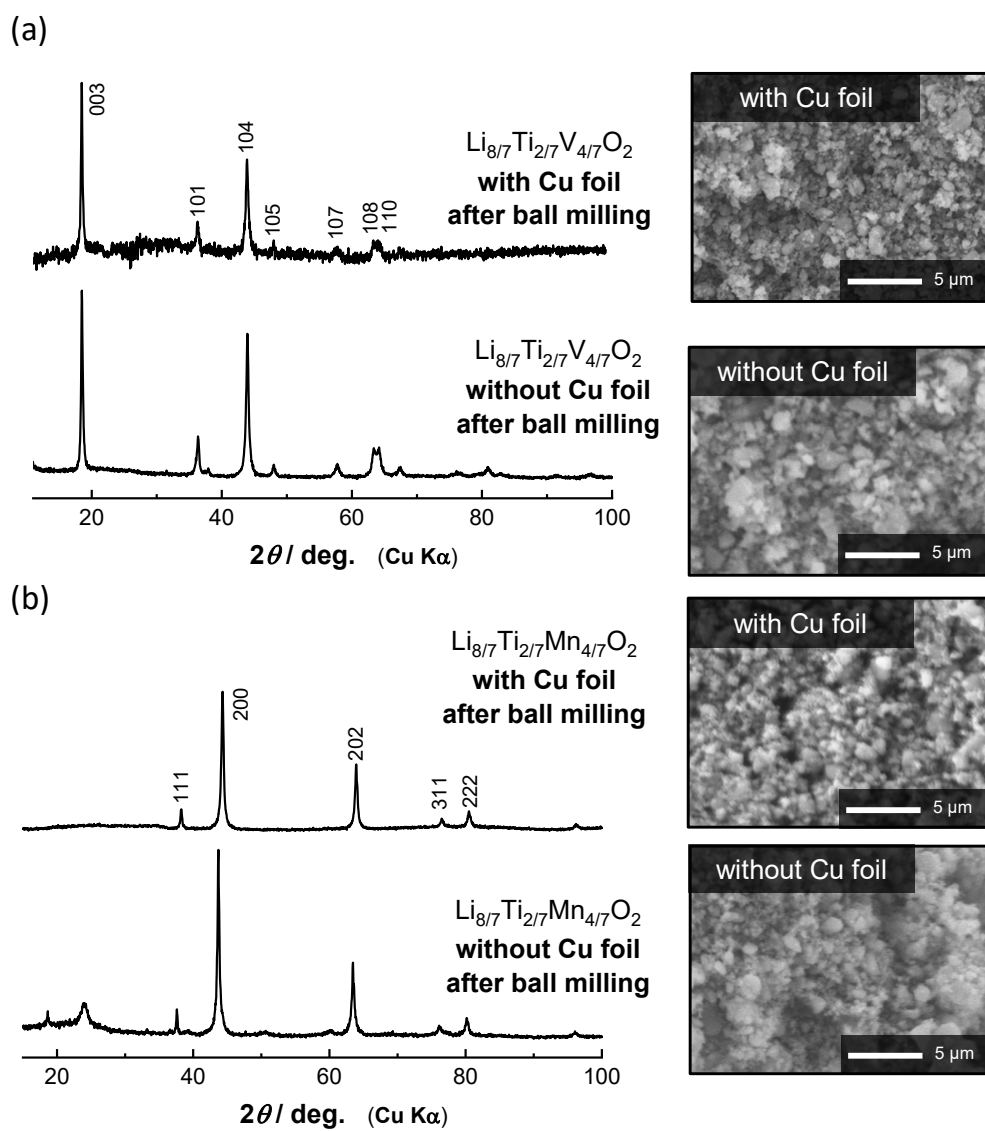


Figure S7. The XRD patterns and SEM images for carbon composited samples of $\text{Li}_{8/7}\text{Ti}_{2/7}\text{V}_{4/7}\text{O}_2$ and $\text{Li}_{8/7}\text{Ti}_{2/7}\text{Mn}_{4/7}\text{O}_2$ synthesized with/without Cu foil.